Proceedings of the 3rd Croatian Conference on Earthquake Engineering - 3CroCEE
19–22 March 2025, Split, Croatia

DOI: https://doi.org/10.5592/CO/3CroCEE.2025.94

ANALYTICAL AND NUMERICAL INVESTIGATION OF THE SITE RESPONSE PERIOD IN THE SAGUENAY REGION, EASTERN CANADA

A S M Fahad Hossain[(1)], Ali Saeidi[(2)], Mohammad Salsabili[(3)], Miroslav Nastev[(4)] and Juliana Ruiz Suescun[(5)]

[(1,2)] *Université du Québec à Chicoutimi, 555 Bd de l'Université, Chicoutimi, QC G7H 2B1, Canada*
[(3)] *University of Western Ontario, 1151 Richmond St, London, ON N6A 3K7, Canada*
[(4)] *Geological Survey of Canada, 490 R. de la Couronne, Québec, QC G1K 9A9, Canada*
[(5)] *Hydro Québec, 75 Boul. René-Lévesque O, Montréal, QC H2Z 1A4, Canada*

Abstract

The fundamental vibration period T_0 is often applied with the standard V_{S30} approach to improve the prediction of the seismic site effects. The commonly used equivalent single-layer method ($4H/V_{Savg}$) usually overestimates T_0. The present study applies a multi-layered method to develop empirical correlations for T_0 prediction. Numerical analyses examine the effects of the soil nonlinearity on T_0 shift and reduction of peak amplitude, establishing correlations for different hazard levels. The Saguenay Lac-Saint-Jean region (SLSJ), characterised by moderate seismicity and a strong impedance contrast at the bedrock interface, was selected as the study area. Results indicate that the analytical approach using the multiple soil layer method considerably reduces the T_0 overestimation. Empirical models were developed for site period evaluation using the multiple soil layer method for elastic strain and nonlinear dynamic response.

Keywords: Fundamental site period, Nonlinear site period, nonlinear analysis.

1. Introduction

The local geological and geotechnical properties of soils may lead to rapid variations of the seismic shaking in terms of duration and amplitudes at certain period ranges. In response to cyclic loading during the strong earthquake motion, the shear strains in soil increase, accompanied by a damping increase causing softening of the soil while reducing the amplitude of the ground motion amplification. This phenomenon contributes to a shift of the fundamental site period (T_0) to longer values, referred to as the nonlinear site period. These so-called seismic site effects were well observed during the 1985 Michoacan and 1989 Loma Prieta earthquakes. [1]. In seismic hazard evaluations, site effects are commonly accounted for with simple site conditions proxies, where the time-averaged shear-wave velocity of the top 30 m (V_{S30}), related to soil stiffness, is considered as the primary site parameter [2]. T_0 is also applied as an indicator of the resonance frequency to help improve surface ground motion prediction. It represents a soil column's most extended natural vibration period and can be determined through field measurements, analytical and empirical solutions, and numerical analysis. [3] and [4], demonstrated the benefits of using dominant periods from H/V spectral ratios (HVSR) for consistent site classification across diverse geologies. [5] refined this approach with H/V response spectra, creating new site categories. Studies by [6] and [7] confirmed HVSR's reliability, revealing sediment thickness effects missed by geology-based methods. [8] expanded HVSR analysis with Spanish data, while recent research employs Fourier and response spectra to calculate dominant periods (e.g., [9]; [10]). [11], [12] used nonlinear site response methods to evaluate the role of soil nonlinearity in shifting site periods. These findings underline the importance of considering nonlinear site periods for accurate seismic site classification. [13] analyzed the existing methods to calculate T_0 from shear-wave velocity V_S using various analytical approaches. The simple characteristic site period approximation $T_0=(4H/V_{Savg})$ is mainly applied when the time-averaged shear-wave velocity (V_{Savg}) and the

DOI: https://doi.org/10.5592/CO/3CroCEE.2025.94

thickness of the soil column (H) are known [14]. However, it tends to overestimate T_0 as the nonlinear soil behavior during earthquakes, where stiffness degradation increases the site period, is not accounted for. Also, the equivalent single layer (ESL) assumption with uniform V_S across thick soil deposits, instead of the common increasing velocity depth gradient, shifts the evaluated T_0 to longer periods [11], [12]. To improve accuracy, [15] proposed the multilayer soil Layer (MSL) approach, building on the work of [16] and [17] to account for variations across layers. Therefore, comparing T_0 across different methods is essential, as ESL is frequently used as a secondary proxy in ground motion equations.

The present study is part of the ongoing site categorization in the Saguenay region, eastern Canada. Located near the Charlevoix-Kamouraska seismic zone, the Saguenay region is exposed to strong earthquakes with a predicted magnitude of up to M7.0 and a 2%/50yrs probability of exceedance (PE). The 1988 M5.9 Saguenay earthquake was the strongest recorded earthquake in eastern North America in more than 50 years, highlighting the need to assess the site response during intense seismic events. The study's objective is to investigate the dynamic site response with a focus on the fundamental site period (T_0). Site responses of 52 typical soil profiles in the study area, exposed to synthetic and recorded strong ground motions, are analyzed and compared to existing analytical models. Predictive T_0 models are developed with ESL and MSL approaches using equivalent linear and nonlinear analyses.

2. Materials and Methods

Saguenay, situated 200 km north of Québec City with a population of 147,100, serves as a central hub for commerce and administration. Positioned within the seismically active Saguenay graben, part of the Charlevoix-Kamouraska seismic zone, the city has experienced significant earthquakes, such as those in 1663 and 1988 with magnitudes of 6.0. The region's bedrock is composed of Precambrian rocks from the Grenville Province. At the same time, the lowlands are layered with glacial and postglacial deposits, including till, glaciofluvial gravel, glaciomarine clay, and deltaic sands, creating a geologically diverse landscape. The selection of 52 soil profiles in this area was based on the vertical and geographic distribution of four surface components: sand, gravel, clay, and till, distributed over four cross-sections shown in Figure 1(a), with thickness details for surface soils in Saguenay. 10 to 15 profiles were retrieved for each cross-section, with 52 stratigraphic soil profiles analyzed. The bedrock was modeled as an elastic half-space with specific density and shear-wave velocity parameters. Two earthquake scenarios, with moment magnitudes of M6 and M7 and exceedance probabilities of 1/975 and 1/2475 years, represented Saguenay's seismic hazard (www.seismotoolbox.ca). Four artificial ground movements were selected based on source-to-site distances of 40–60 km, and two accurate earthquake records from eastern Canada were incorporated: the 1988 M5.9 Saguenay earthquake (35 km from the epicenter) and the 2010 M5.1 Val-des-Bois earthquake (22 km from the epicenter). Figure 1(b) illustrates initial acceleration time histories for each ground movement, scaled to target spectra using the SeismoMatch software (www.seismosoft.com/). All site-specific soil properties used in the analysis are shown in Table 1.

The site response analysis was carried out on 52 soil profiles, using six input ground motions, each scaled to five earthquake hazard levels: 2%/50yrs, 3.5%/50yrs, 5%/50yrs, 10%/50yrs and 20%/50yrs PE from NBCC 2020. This analysis employed nonlinear methods in the time domain and equivalent linear methods in the frequency domain. The open-source software DEEPSOIL v7.0 was used and recognized for its reliability in site response analysis. Earlier versions of DEEPSOIL have been extensively validated and shown to replicate observed responses in well-documented soil sites accurately. In DEEPSOIL, the MKZ hyperbolic model, which accounts for pressure dependency, was applied to simulate modulus reduction and shear stress characteristics. The software technical guidelines provide an overview of the methods used for calculating the site response of a soil column discretized into individual layers using a single-

DOI: https://doi.org/10.5592/CO/3CroCEE.2025.94

or multi-degree-of-freedom system and solving the dynamic equilibrium equations. Seismic amplification is the ratio of calculated surface to bedrock response spectral accelerations in time domain solution or Fourier amplitude spectrum ratio from frequency domain solution. The final amplification factor for each model was determined by taking the geometric mean of six responses obtained from different earthquake motions at the surface.

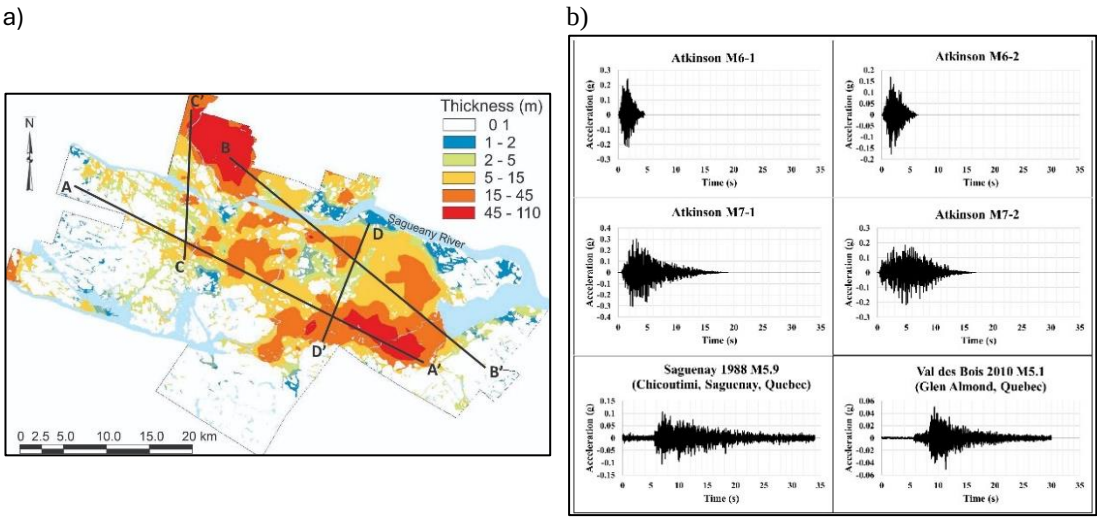

Figure 1. a) Thickness of surficial deposits with four cross-sections for selection of the 52 soil profiles used in the site response analyses (modified from [18] and b) unscaled input time histories.

Table 1. Adopted geotechnical and dynamic properties of soils and rock in the Saguenay region.

	Shear-Wave Velocity vs. Depth (m/s)	Density (kN/m^3)	Shear Modulus Reduction and Damping Ratio curves
Clay	Vs = 114.5 + 9.4 x D$^{0.76}$ [19]	18.7 [20]	[21]
Sand	Vs = 144.9 + 2.55 x D [19]	17.5 [20]	[22]*
Gravel	Vs = 46.861 + 61.55 x D$^{0.5}$ [19]	18.3 [23]*	[24]*
Till	V_{Still} = 582, σ=±174 (Motazedian et al., 2011)	21.0 [26]	Hydro Quebec (internal communication)
Rock	V_{Srock} = 1875, σ=±781 [27]	28.0 [28]	N/A

* Studies conducted in other regions

3. Analytical approach

The fundamental site period of 52 typical vertical profiles was calculated using both the equivalent single layer (ESL; T_0=4H/Vs) and multiple soil layers (MSL) approaches as described in Hadjian (2002). The procedure for calculating the T_0 in MSL profiles is described with equations 1 to 3. The process starts by considering the top two layers with respective fundamental periods T_1 and T_2. The combined fundamental period $T_{i=1}$ of these two layers is determined. In the next step, these two layers are treated as a single layer, and the third layer underneath is incorporated to calculate the combined $T_{i=2}$. This process is repeated iteratively across all the layers until the final T_0 is calculated for each of the 52 soil profiles. The number of iterations equals the number of assumed layers minus 1.

$$\frac{T}{T_1} = \sqrt{\frac{\pi^2}{8}\left[0.75 + \left(\frac{T_2}{T_1}\right)^2\left(1 + 2\frac{H_1}{H_2}\right)\right]} \quad ; \quad \left[\text{For } \frac{T_2}{T_1} > 0.1, H_1 > H_2\right] \tag{1}$$

DOI: https://doi.org/10.5592/CO/3CroCEE.2025.94

$$\frac{T}{T_1} = \left[1 + \beta\left(\frac{T_2}{T_1}\right)^n \left(1 + 2\frac{H_1}{H_2}\right)^n\right]^{\frac{1}{n}} \quad ; \quad \left[\text{For } \frac{T_2}{T_1} > 0.1, H_1 \leq H_2\right] \tag{2}$$

$$\frac{T}{T_1} = \left[1 + \frac{H_1}{H_2}\left(\frac{T_2}{T_1}\right)^2\right] \quad ; \quad \left[\text{For } \frac{T_2}{T_1} \leq 0.1\right] \tag{3}$$

where, $\beta = 1\text{-}0.2\left(\frac{H_1}{H_2}\right)^2$; and $n = 4 - 1.8\frac{H_1}{H_2}$

At the end of the process, an empirical correlation was developed to convert the fundamental site period from TESL to TMSL, as shown in equation 4.

$$T_{MSL} = 0.87 * T_{ESL}^{0.93}; \quad R^2 = 1.00; \quad \sigma = 0.018 \tag{4}$$

The calculated and empirical fundamental site period in multiple soil layered methods is plotted against the calculated site fundamental period in equivalent single-layer methods, as shown in Figure 2. It can be seen in Figure 2 that the fundamental site period calculated using MSL is lower than that using ESL and that the difference increases for soil columns with higher fundamental periods.

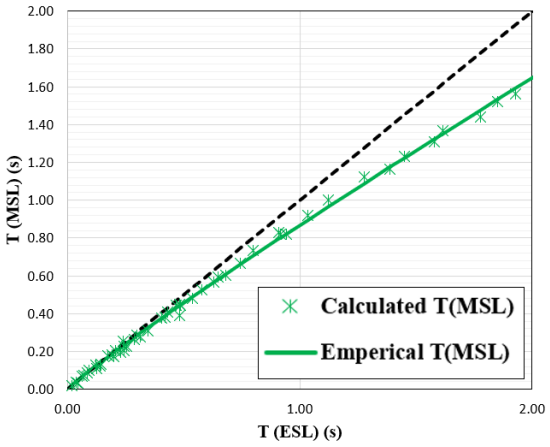

Figure 2. Correlation between the fundamental site periods obtained using the equivalent single layer, T_{ESL}, and the multiple TMSL approaches of soil layering. The black dashed line indicates the 1:1 correlation, where $T_{MSL}=T_{ESL}$.

4. Nonlinear numerical modelling

In response to cyclic loading during the strong earthquake motion, the shear strains in soil increase, accompanied by a damping increase causing softening of the soil and reducing the amplitude of the ground motion amplification. This phenomenon contributes to a shift of the fundamental site period (T_0) to longer values, which becomes more significant for stronger earthquake motions. Nonlinear site response simulations were carried out with the DEEPSOIL software to evaluate the magnitude of the period shift. The results are compared to the standard T_{ESL}. Two sets of 6 ground motions (Figure 1b) were scaled according to the NBCC 2020 hazard for the Saguenay region with a probability of exceedance (PE in the further text) of 2%/50yrs, which corresponds to a return period of 2475yr, and 10%/50yrs PE (475yr; NBCC2020). The nonlinear site period, T_{NL}, was determined from the acceleration response spectra at the ground surface for the period with maximum spectral amplification. The results are shown in Figure 3.

DOI: https://doi.org/10.5592/CO/3CroCEE.2025.94

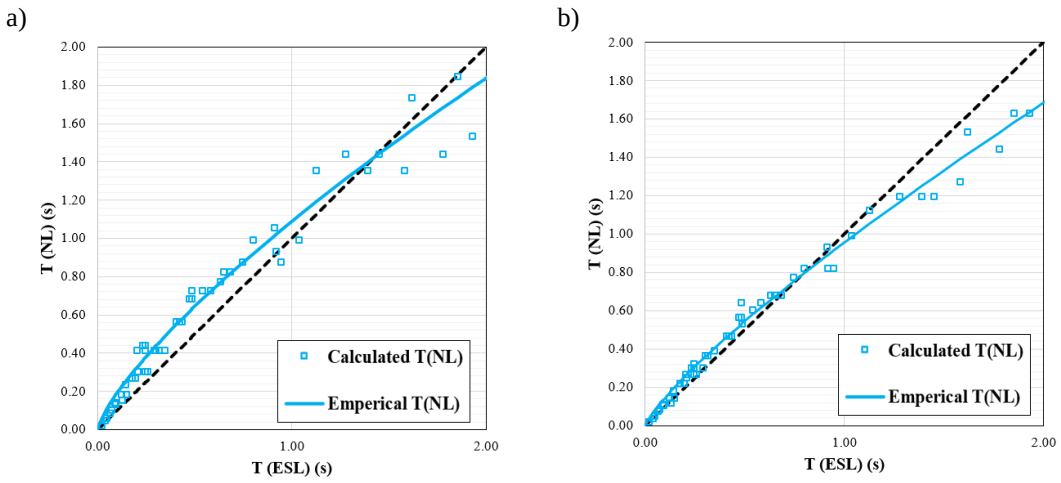

Figure 3. Nonlinear site period of soil for ground motion with a) 2%/50yrs PE and b) 10%/50yrs PE. The black dashed line indicates 1:1 correlation, where T_{NL}=T_{ESL}.

Figure 3 indicates that in the short period range, T_{NL} is higher than T_{ESL} for both hazard levels and shifts toward longer periods. In the longer period ranges, it becomes lower than T_{ESL}. The shift below the 1:1 line first occurs for ground motions scaled to 10%/50yrs PE, at approximately T=0.7s, and then for the ground motions scaled to 2%/50yrs PE, at approximately T=2.0s. Such performance can be explained by the conventional ESL method, which tends to overestimate T_0 values, especially for thicker soil columns. On the other hand, the MSL method provides better T_0 estimates. Also, soil columns with higher V_{Savg} display higher stiffness, resulting in a smaller T_0 shift due to earthquake loading compared to softer soil columns. For both sets of input motions, empirical correlations were developed as described with equations 5 and 6 for 2%/50yrs and 10%/50yrs PE, respectively. Additionally, a relationship between the nonlinear site period T_{NL}, on one hand side, and the peak ground acceleration (PGA) and the fundamental site period (T_0), on the other, was developed considering all five hazard levels with PE of 2%, 3.5%, 5%/, 10% and 20% in 50yrs, equation 7.

$$T_{NL\text{-}2\%/50yrs\ PE} = 1.09 * T_{ESL}^{0.76}; \quad R^2 = 0.97; \quad \sigma = 0.093 \qquad (5)$$

$$T_{NL\text{-}10\%/50yrs\ PE} = 0.96 * T_{ESL}^{0.82}; \quad R^2 = 0.99; \quad \sigma = 0.047 \qquad (6)$$

$$T_{NL} = 1.28 * PGA^{0.14} * T_{ESL}^{0.92}; \quad R^2 = 0.98; \quad \sigma = 0.086 \qquad (7)$$

Figure 4 shows the scatter of nonlinear site period results from all five hazards with the fundamental site periods T(ESL) and T(MSL). In all empirical correlations, the R^2 value is close to 1, indicating low errors in the regression analysis.

In the numerical site response modeling process, it is important to conduct an equivalent linear analysis to compare and validate the results of the nonlinear analysis. To this end, the amplification values were calculated as the ratio between the ground surface acceleration response spectra and Fourier amplitude spectra and their analogs of the input ground motions. In both cases, the site periods were determined to correspond to the maximum amplification. The site period in the frequency domain analysis was defined as the reciprocal value of the frequency. Figures 5 and 6 compare maximum amplification values and the corresponding site periods from the response spectrum using a time-domain nonlinear approach (NL) and

Proceedings of the 3rd Croatian Conference on Earthquake Engineering - 3CroCEE
19–22 March 2025, Split, Croatia

DOI: https://doi.org/10.5592/CO/3CroCEE.2025.94

frequency-domain equivalent linear analysis (EL) corresponding to 2%/50-year and 10%/50-year PE hazard scenarios.

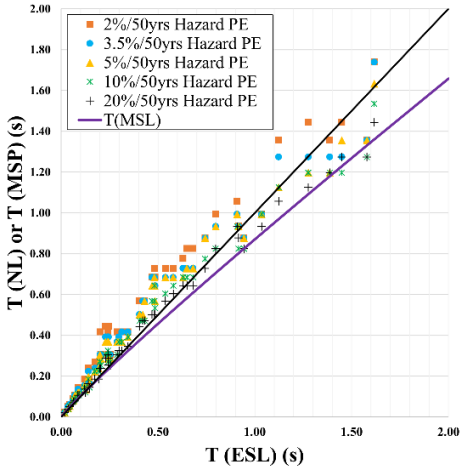

Figure 4. The scatter of nonlinear site periods T(NL) from different soil models for all five hazard levels and T(MSL) against the fundamental site periods T(ESL). The black dashed line indicates a 1:1 correlation, where T_{NL} or T_{MSL}=T_{ESL}.

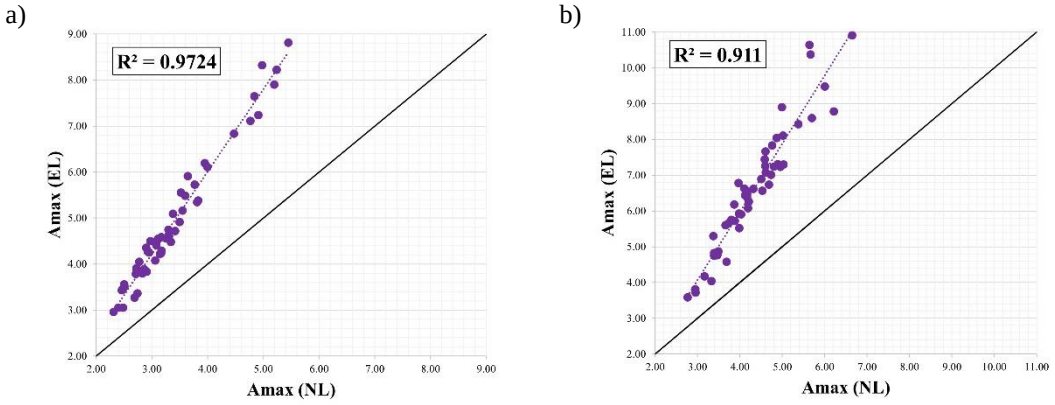

Figure 5. Comparison of the maximum amplifications from nonlinear, Amax (NL), and equivalent linear, Amax (EL), analyses for: a) 2%/50yrs PE and b) 10%/50yrs PE. (Black straight line is the 1:1 line where Amax (EL)=Amax (NL))

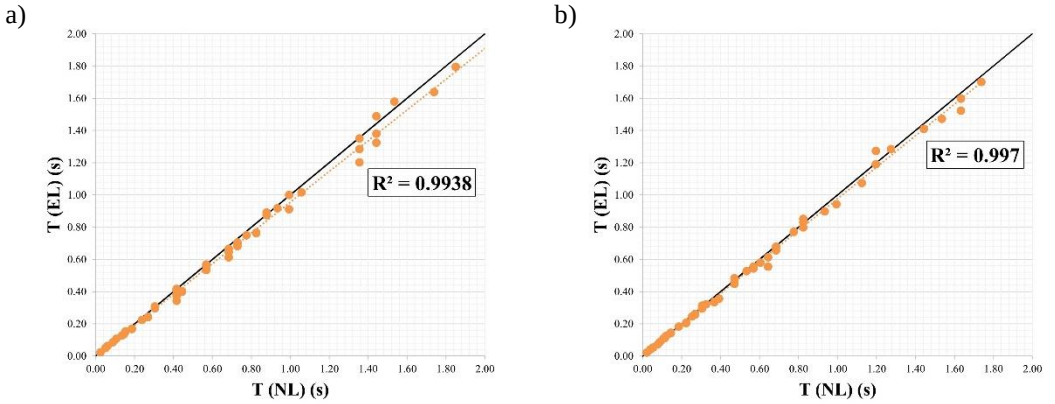

Figure 6. Comparison of the maximum amplification and corresponding site periods from nonlinear, T_{NL}, and equivalent linear, T_{EL}, analyses for a) 2%/50yrs PE and b) 10%/50yrs PE. (Black straight line is the 1:1 line where Amax (EL)=Amax (NL))

DOI: https://doi.org/10.5592/CO/3CroCEE.2025.94

The results in Figures 4 and 5 demonstrate high correlations between the maximum amplifications and fundamental site periods, with R2 values ranging from 0.91 to 0.99 for both hazard levels. Slightly higher deviations among the data points can be observed for higher amplifications and longer periods. These results suggest a stable and predictable relationship between nonlinear and equivalent linear analyses across both hazard scenarios.

5. Resonance Effect

In soil dynamics, the resonance effect occurs when the dominant period range of the incoming seismic waves, where most of the earthquake energy is concentrated, aligns with the fundamental site period or the natural frequency of the soil column. This alignment contributes to amplified seismic shaking at the ground surface. The buildup in the soil vibrations amplitude can potentially lead to permanent soil deformations, such as subsidence, lateral spread, landslide, etc. Site response analyses indicate that maximum amplification occurs when the ratio between the dominant input vibration period and the site response period becomes close or equal to 1 [29]. Here, most of the earthquake energy content is concentrated in the dominant input vibration period. The site response period refers to the maximum period at which the soil vibrates, with T_0 indicating low (elastic) strain conditions and T_{NL} indicating nonlinear soil behavior under earthquake loading. The nonlinear amplification values were plotted with respect to the ratio of the oscillation period and site period, as shown in Figure 7.

The nonlinear analysis correlated against the vibration period to fundamental site period ratio in Figure 7a indicates that a shift in the resonance period occurs due to the considered nonlinearity. However, when nonlinear amplification is compared against the ratio of the oscillation period (T_{osc}) to the nonlinear site period (T_{NL}) derived from the empirical models discussed in section 4, resonance occurs steadily near the ratio of 1 (Figure 7b).

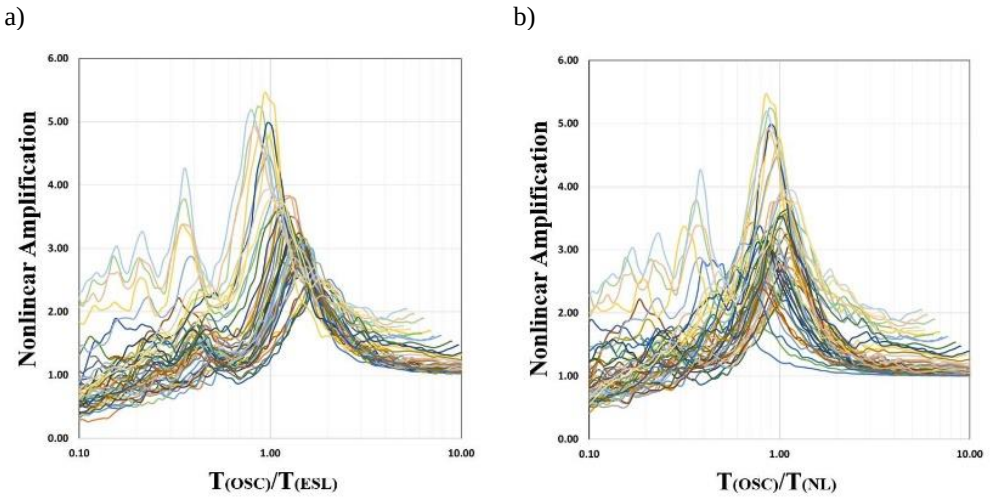

Figure 7. Amplification Values vs. Ratio of Vibration Period to Site Natural Period for 2%/50yrs PE: a) a) Nonlinear amplification vs T_{osc}/T_{ESL} b) Nonlinear amplification vs T_{osc}/T_{NL}.

6. Conclusion

A comprehensive 1D site response analysis was conducted in the Saguenay region on 52 soil profiles with site-specific properties. Both the nonlinear time-domain and the equivalent linear frequency-domain methods were used. This analysis employed hazard levels of 2%, 3.5%, 5%,

DOI: https://doi.org/10.5592/CO/3CroCEE.2025.94

10% and 20% probability of exceedance in 50 years as specified in NBCC2020. Results from both time-domain and frequency-domain methods align well, validating the findings.

Each soil column's fundamental site period was calculated using the widely used equivalent single-layer method and a multiple-soil-layer profile method. The multiple-layer method was observed to be more effective, resulting in less overestimation of the fundamental site period. We developed an empirical correlation for the multiple-layer method, enabling precise calculation of the fundamental site period from the commonly used single-layer method.

Additionally, we calculated the nonlinear site period from the site response analysis by identifying the maximum amplification and developing empirical models for different hazard levels. We highlighted the resonance effect in the Saguenay region, which is critical as it may amplify the amplitudes of the ground motion and cause site-induced damage due to resonance. An amplification model incorporating nonlinear site response and accounts for the resonance effect using the nonlinear site period is essential for accurate assessment in this region.

References

[1] J. H. Steidl, “Site Response in Southern California for Probabilistic Seismic Hazard Analysis,” Bulletin of the Seismological Society of America, vol. 90, no. 6B, pp. S149–S169, Dec. 2000, doi: 10.1785/0120000504.

[2] A. F. Hossain, A. Saeidi, M. Salsabili, M. Nastev, and J. Suescun, “Soil Dynamic Response and Site Amplification Parameters for Saguenay, Eastern Canada,” Japanese Geotechnical Society Special Publication, vol. 10, no. 52, p. v10.OS-41-03, 2024, doi: 10.3208/jgssp.v10.OS-41-03.

[3] J. X. Zhao et al., “An empirical site-classification method for strong-motion stations in Japan using H/V response spectral ratio,” Bulletin of the Seismological Society of America, vol. 96, no. 3, pp. 914–925, Jun. 2006, doi: 10.1785/0120050124.

[4] Y. Fukushima, L. F. Bonilla, O. Scotti, and J. Douglas, “Site Classification Using Horizontal-to-vertical Response Spectral Ratios and its Impact when Deriving Empirical Ground-motion Prediction Equations,” Journal of Earthquake Engineering, vol. 11, no. 5, pp. 712–724, Oct. 2007, doi: 10.1080/13632460701457116.

[5] C. Di Alessandro, L. F. Bonilla, D. M. Boore, A. Rovelli, and O. Scotti, “Predominant-Period Site Classification for Response Spectra Prediction Equations in Italy,” Bulletin of the Seismological Society of America, vol. 102, no. 2, pp. 680–695, Apr. 2012, doi: 10.1785/0120110084.

[6] N. Harinarayan and A. Kumar, “Seismic Site Classification of Recording Stations in Tarai Region of Uttarakhand, from Multiple Approaches,” Geotechnical and Geological Engineering, vol. 36, no. 3, pp. 1431–1446, Jun. 2018, doi: 10.1007/s10706-017-0399-1.

[7] S. Chopra, V. Kumar, P. Choudhury, and R. B. S. Yadav, “Site classification of Indian strong motion network using response spectra ratios,” J Seismol, vol. 22, no. 2, pp. 419–438, Mar. 2018, doi: 10.1007/s10950-017-9714-9.

[8] L. A. Pinzón, L. G. Pujades, A. Macau, E. Carreño, and J. M. Alcalde, “Seismic Site Classification from the Horizontal-to-Vertical Response Spectral Ratios: Use of the Spanish Strong-Motion Database,” Geosciences (Basel), vol. 9, no. 7, p. 294, Jul. 2019, doi: 10.3390/geosciences9070294.

[9] H. Ghofrani, G. M. Atkinson, and K. Goda, “Implications of the 2011 M9.0 Tohoku Japan earthquake for the treatment of site effects in large earthquakes,” Bulletin of Earthquake Engineering, vol. 11, no. 1, pp. 171–203, Feb. 2013, doi: 10.1007/s10518-012-9413-4.

DOI: https://doi.org/10.5592/CO/3CroCEE.2025.94

[10] H. Livaoğlu, E. Şentürk, and F. Sertçelik, "A Comparative Study of Response and Fourier Spectral Ratios on Classifying Sites," Pure Appl Geophys, vol. 178, no. 5, pp. 1745–1759, May 2021, doi: 10.1007/s00024-021-02722-1.

[11] D. Motazedian, K. Khaheshi Banab, J. A. Hunter, S. Sivathayalan, H. Crow, and G. Brooks, "Comparison of Site Periods Derived from Different Evaluation Methods," Bulletin of the Seismological Society of America, vol. 101, no. 6, pp. 2942–2954, Dec. 2011, doi: 10.1785/0120100344.

[12] D. Motazedian, H. Torabi, J. A. Hunter, H. L. Crow, and M. Pyne, "Seismic site period studies for nonlinear soil in the city of Ottawa, Canada," Soil Dynamics and Earthquake Engineering, vol. 136, p. 106205, Sep. 2020, doi: 10.1016/j.soildyn.2020.106205.

[13] S. Wang, Y. Shi, W. Jiang, E. Yao, and Y. Miao, "Estimating Site Fundamental Period from Shear-Wave Velocity Profile," Bulletin of the Seismological Society of America, vol. 108, no. 6, pp. 3431–3445, Dec. 2018, doi: 10.1785/0120180103.

[14] A. F. Hossain, M. Salsabili, A. Saeidi, J. R. Suescun, and M. Nastev, "Effects of Shear Wave Velocity and Thickness of Soil Layers on 1D Dynamic Response in the Saguenay Region, Quebec," in Rocscience International Conference (RIC 2023), Toronto: Atlantis Press, 2023, pp. 165–173. doi: 10.2991/978-94-6463-258-3_17.

[15] A. H. Hadjian, "Fundamental period and mode shape of layered soil profiles," Soil Dynamics and Earthquake Engineering, vol. 22, no. 9–12, pp. 885–891, Oct. 2002, doi: 10.1016/S0267-7261(02)00111-2.

[16] Madera G., "Fundamental period and amplification of peak acceleration in layered systems," 1970.

[17] Dobry, R., Oweis, I., & Urzua, A. (1976). Simplified procedures for estimating the fundamental period of a soil profile. Bulletin of the Seismological Society of America, 66(4), 1293-1321.

[18] M. Salsabili, A. Saeidi, A. Rouleau, and M. Nastev, "Development of empirical CPTu-V correlations for post-glacial sediments in Southern Quebec, Canada, in consideration of soil type and geological setting," Soil Dynamics and Earthquake Engineering, vol. 154, p. 107131, Mar. 2022, doi: 10.1016/j.soildyn.2021.107131.

[19] M. Salsabili, A. Saeidi, A. Rouleau, and M. Nastev, "Probabilistic approach for seismic microzonation integrating 3D geological and geotechnical uncertainty," Earthquake Spectra, vol. 39, no. 1, pp. 310–334, Feb. 2023, doi: 10.1177/87552930221132576.

[20] A.-G. Sanou, A. Saeidi, S. Heidarzadeh, R. V. P. Chavali, H. E. Samti, and A. Rouleau, "Geotechnical Parameters of Landslide-Prone Laflamme Sea Deposits, Canada: Uncertainties and Correlations," Geosciences (Basel), vol. 12, no. 8, p. 297, Jul. 2022, doi: 10.3390/geosciences12080297.

[21] M. Abdellaziz et al., "New model of shear modulus degradation and damping ratio curves for sensitive Canadian clays," Canadian Geotechnical Journal, vol. 60, no. 6, pp. 784–801, Jun. 2023, doi: 10.1139/cgj-2021-0475.

[22] EPRI, "Guidelines for Site Specific Ground Motions," 1993.

[23] K. M. Rollins, M. D. Evans, N. B. Diehl, and W. D. D. III, "Shear Modulus and Damping Relationships for Gravels," Journal of Geotechnical and Geoenvironmental Engineering, vol. 124, no. 5, pp. 396–405, May 1998, doi: 10.1061/(ASCE)1090-0241(1998)124:5(396).

DOI: https://doi.org/10.5592/CO/3CroCEE.2025.94

[24] H. B. Seed, R. T. Wong, I. M. Idriss, and K. Tokimatsu, "Moduli and Damping Factors for Dynamic Analyses of Cohesionless Soils," Journal of Geotechnical Engineering, vol. 112, no. 11, pp. 1016–1032, Nov. 1986, doi: 10.1061/(ASCE)0733-9410(1986)112:11(1016).

[25] D. Motazedian, J. A. Hunter, A. Pugin, and H. Crow, "Development of a Vs 30 (NEHRP) map for the city of Ottawa, Ontario, Canada," Canadian Geotechnical Journal, vol. 48, no. 3, pp. 458–472, Mar. 2011, doi: 10.1139/T10-081.

[26] R. Urgeles, J. Locat, H. J. Lee, and F. Martin, "The Saguenay Fjord, Quebec, Canada: integrating marine geotechnical and geophysical data for spatial seismic slope stability and hazard assessment," Mar Geol, vol. 185, no. 3–4, pp. 319–340, Jun. 2002, doi: 10.1016/S0025-3227(02)00185-8.

[27] S. Ladak, S. Molnar, and S. Palmer, "Multi-method site characterization to verify the hard rock (Site Class A) assumption at 25 seismograph stations across Eastern Canada," Earthquake Spectra, vol. 37, no. 1_suppl, pp. 1487–1515, Jul. 2021, doi: 10.1177/87552930211001076.

[28] A. Saeidi, S. Heidarzadeh, S. Lalancette, and A. Rouleau, "The effects of in situ stress uncertainties on the assessment of open stope stability: Case study at the Niobec Mine, Quebec (Canada)," Geomechanics for Energy and the Environment, vol. 25, p. 100194, Mar. 2021, doi: 10.1016/j.gete.2020.100194.

[29] J. Harmon et al., "Site Amplification Functions for Central and Eastern North America – Part I: Simulation Data Set Development," Earthquake Spectra, vol. 35, no. 2, pp. 787–814, May 2019, doi: 10.1193/091017EQS178M.